# Conformationally Constrained, Stable, Triplet Ground State ($S = 1$) Nitroxide Diradicals. Antiferromagnetic Chains of $S = 1$ Diradicals

Andrzej Rajca,*,[†] Masahiro Takahashi,[†] Maren Pink,[‡] Gaëlle Spagnol,[†] and Suchada Rajca[†]

*Contribution from the Department of Chemistry, University of Nebraska, Lincoln, Nebraska 68588-0304, and IUMSC, Department of Chemistry, Indiana University, Bloomington, Indiana 47405-7102*

Received February 22, 2007; E-mail: arajca1@unl.edu

***Abstract:*** Nitroxide diradicals, in which nitroxides are annelated to *m*-phenylene forming tricyclic benzo-bisoxazine-like structures, have been synthesized and characterized by X-ray crystallography, magnetic resonance (EPR and $^1$H NMR) spectroscopy, as well as magnetic studies in solution and in solid state. For the octamethyl derivative of benzobisoxazine nitroxide diradical, the conformationally constrained nitroxide moieties are coplanar with the *m*-phenylene, leading to large values of $2J$ ($2J/k > 200$ K in solution and $2J/k \gg 300$ K in the solid state). For the diradical, in which all ortho and para positions of the *m*-phenylene are sterically shielded, distortion of the nitroxide moieties from coplanarity is moderate, such that the singlet–triplet gaps remain large in both solution ($2J/k > 200$ K) and the solid state ($2J/k \approx 400-800$ K), though an onset of thermal depopulation of the triplet ground state is detectable near room temperature. These diradicals have robust triplet ground states with strong ferromagnetic coupling and good stability at ambient conditions. Magnetic behavior of the nitroxide diradicals at low temperature is best fit to the model of one-dimensional $S = 1$ Heisenberg chains with intrachain antiferromagnetic coupling. The antiferromagnetic coupling between the $S = 1$ diradicals may be associated with the methyl nitroxide C−H- - -O contacts, including nonclassical hydrogen bonds. These unprecedented organic $S = 1$ antiferromagnetic chains are highly isotropic, compared to those of the extensively studied Ni(II)-based chains.

## Introduction

Stable triplet ground state ($S = 1$) diradicals with strong ferromagnetic coupling have attracted great interest as building blocks in the design of organic and organometallic magnetic materials, as well as in the development of new agents for biomedical applications.[1-8] Most of the stable $S = 1$ diradicals reported to date are based on sterically hindered and confor-mationally unrestricted *tert*-alkylnitroxides that are cross-conjugated through *m*-phenylene, in which their intrinsic properties, such as ferromagnetic coupling and stability, can be modulated by simple structural modifications.[9-11] These diradicals may possess a singlet–triplet energy gap ($2J$), exceeding or comparable to the thermal energy at room temperature. However, under practical conditions, that is, when associated with transition-metal ions to form coordination polymers (organometallic magnetic materials) or with highly polar aqueous solutions/media in biomedical applications, the nitroxides are twisted out of the plane of the *m*-phenylene,[2,9,10,12] leading to weak paramagnetic properties, that is, small values of $|2J|$, at room temperature.[13-17]

† University of Nebraska.

‡ Indiana University.

(1) (a) Iwamura, H.; Koga, N. *Acc. Chem. Res.* **1993**, *26*, 346−351. (b) Rajca, A. *Chem. Rev.* **1994**, *94*, 871−893. (c) *Magnetic Properties of Organic Materials;* Lahti, P. M., Ed.; Marcel Dekker: New York, 1999. (d) *Molecular Magnetism;* Itoh, K., Kinoshita, M., Eds.; Gordon and Breach: Amsterdam, 2000. (e) Rajca, A. *Chem.−Eur. J.* **2002**, *8*, 4834−4841. (f) Rajca, A. *Adv. Phys. Org. Chem.* **2005**, *40*, 153−199. (g) Shishlov, N. M. *Russ. Chem. Rev.* **2006**, *75*, 863−884.

(2) (a) Iwamura, H.; Inoue, K.; Kaga, N. *New J. Chem.* **1998**, 201−210. (b) Inoue, K. *Struct. Bonding* **2001**, *100*, 61−91.

(3) (a) Rajca, A.; Wongsriratanakul, J.; Rajca, S. *Science* **2001**, *294*, 1503−1505. (b) Rajca, S.; Rajca, A.; Wongsriratanakul, J.; Butler, P.; Choi, S. *J. Am. Chem. Soc.* **2004**, *126*, 6972−6986. (c) Rajca, A.; Wongsriratanakul, J.; Rajca, S. *J. Am. Chem. Soc.* **2004**, *126*, 6608−6626. (d) Rajca, A.; Wongsriratanakul, J.; Rajca, S.; Cerny, R. L. *Chem.−Eur. J.* **2004**, *10*, 3144−3157. (e) Rajca, A.; Shiraishi, K.; Vale, M.; Han, H.; Rajca, S. *J. Am. Chem. Soc.* **2005**, *127*, 9014−9020.

(4) (a) Fukuzaki, E.; Nishide, H. *J. Am. Chem. Soc.* **2006**, *128*, 996−1001. (b) Fukuzaki, E.; Nishide, H. *Org. Lett.* **2006**, *8*, 1835−1838.

(5) Winalski, C. S.; Shortkroff, S.; Mulkern, R. V.; Schneider, E.; Rosen, G. M. *Magn. Reson. Med.* **2002**, *48*, 965−972.

(6) Lurie, D. J.; Maeder, K. *Adv. Drug Delivery Rev.* **2005**, *57*, 1171−1190.

(7) Li, H.; He, G.; Deng, Y.; Kuppusamy, P.; Zweier, J. L. *Magn. Reson. Med.* **2006**, *55*, 669−675.

(8) Matsumoto, K.; Hyodo, F.; Matsumoto, A.; Koretsky, A. P.; Sowers, A. L.; Mitchell, J. B.; Krishna, M. C. *Clin. Cancer Res.* **2006**, *12*, 2455−2462.

(9) Spagnol, G.; Shiraishi, K.; Rajca, S.; Rajca, A. *Chem. Commun.* **2005**, 5047−5049.

(10) Calder, A.; Forrester, A. R.; James, P. G.; Luckhurst, G. R. *J. Am. Chem. Soc.* **1969**, *91*, 3724−3727.

(11) Volodarsky, L. B.; Reznikov, V. A.; Ovcharenko, V. I. *Synthetic Chemistry of Stable Nitroxides;* CRC Press: Boca Raton, FL, 1994.

(12) The effect of organic matrixes on exchange coupling in trimethylene-based bis(semiquinone) diradicals: Shultz, D. A.; Boal, A. K.; Farmer, G. T. *J. Am. Chem. Soc.* **1997**, *119*, 3846−3847.

(13) Dvolaitzky, M.; Chiarelli, R.; Rassat, A. *Angew. Chem., Int. Ed. Engl.* **1992**, *31*, 180−181.

(14) Kanno, F.; Inoue, K.; Koga, N.; Iwamura, H. *J. Am. Chem. Soc.* **1993**, *115*, 847−850.
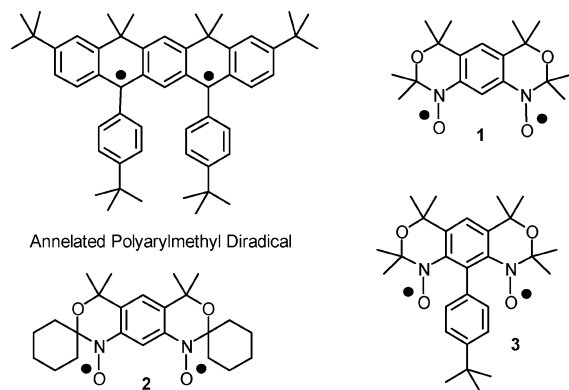
**Figure 1.** Annelated $S = 1$ diradicals.

Annelations of the nitroxide moieties to the *m*-phenylene, such that the nitroxides are conformationally constrained to coplanarity with the *m*-phenylene, may provide diradicals with large 2*J* values that are relatively insensitive to environmental perturbations. To our knowledge, there are only two known annelated $S = 1$ organic diradicals: the annelated polyarylmethyl diradical[18] and nitroxide diradical **1** (Figure 1).[19] The annelated polyarylmethyl diradical was reported to be stable at ambient temperature but reacted with atmospheric oxygen to give peroxides.[20] Nitroxide diradical **1** was reported to be stable in the solid state but decomposed slowly in solution.[19] Furthermore, contradictory magnetic properties of diradical **1**, concerning the ground state and value of 2*J*, were reported.[21]

Intrigued by these results, we set out to investigate further magnetic properties of the annelated nitroxide diradical **1**. In addition, we designed nitroxide diradicals **2** and **3** to probe the effect of steric hindrance on stability and magnetic properties of annelated diradicals. In **2**, spirocyclohexyl groups may provide greater steric shielding of the nitroxides, compared to that in **1**.[22] Substitution with the bulky *tert*-butylphenyl group at the ortho/ortho position, where significant spin density is expected by delocalization from both nitroxides, may provide improved stability or persistence for diradical **3**.[23] However, this steric hindrance may lead to a strained structure and decrease the degree of planarity of the benzobisoxazine annelated system. Therefore, both stability of the diradical and the strength of ferromagnetic coupling may be affected.

We were able to optimize the synthesis to obtain **1** and **3** in good yields and with high purity. This allowed us to carry out a thorough magnetic and structural characterization of both

diradicals. *Most importantly, we discovered unprecedented organic one-dimensional (1-D) antiferromagnetic chains in polycrystalline diradicals **1** and **3**, in which the antiferromagnetic interactions between S = 1 diradicals are mediated through methyl nitroxide C−H- - -O contacts, including nonclassical hydrogen bonds.*[24]

One-dimensional, highly isotropic, antiferromagnetically coupled Heisenberg chains with integer local spins (e.g., $S = 1$) are of fundamental interest.[25−29] In 1983, Haldane conjectured that the ground state of the 1-D Heisenberg model strongly depends on the value of *S* of local spins. In particular, a large energy gap (Haldane gap) between the singlet spin liquid ground state and the lowest triplet excited state was predicted for integer spin Heisenberg antiferromagnetic chains.[25] The Haldane gap was later experimentally confirmed in the study of [Ni(ethylene diamine)$_2$(NO$_2$)](ClO$_4$), abbreviated as NENP.[30] However, the local magnetic anisotropy associated with the Ni(II) ion introduces additional energy gaps, comparable in magnitude to the isotropic Haldane gap,[31] and therefore presents an obstacle to the characterization of the spin excitation spectrum.[32] With the triplet ground state nitroxide diradicals as $S = 1$ local spins, we expect that the organic chains would possess much lower local magnetic anisotropy, thus providing properties that resemble those of isotropic Heisenberg chains. Such intrinsically isotropic chains with $S = 1$ local spins would serve as alternative systems to better understanding of low-dimensional magnetism, as well as the recent topic of quantum spin liquids.[29]

## Results and Discussion

**Synthesis.** The synthesis of diradicals **1**, **2**, and **3** is outlined in Scheme 1.

Starting with dimethyl 4,6-dibromoisophtalate **4** (Supporting Information), the C−N cross-coupling with excess of benzylamine is followed by the reductive debenzylation to give dimethyl 4,6-diaminoisophtalate **6**[33] in high yield. Reaction of **6** with an excess of CH$_3$MgBr provides a diol diamine **7**. Acetic acid-catalyzed condensations of **7** with acetone and cyclohexanone lead to tricyclic diamines **8** and **9**, respectively.[34]

Functionalization of **8** with 4-*tert*-butylphenyl group at the ortho position (with respect to amines) is carried out in two steps. Bromination of **8** with NBS at low temperature gives the monobrominated product **10** in high yield. The Suzuki cross-

(15) Fang, S.; Lee, M.-S.; Hrovat, D. A.; Borden, W. A. *J. Am. Chem. Soc.* **1995**, *117*, 6727−6731.

(16) Rajca, A.; Lu, K.; Rajca, S.; Ross, C. R., II. *J. Chem. Soc., Chem. Commun.* **1999**, 1249−1250.

(17) There is no detailed quantitative experimental data on the dependence of the exchange coupling vs torsional angles in *m*-phenylene moiety. However, a "Karplus−Conroy-type" relationship for exchange coupling in trimethylene-based bis(semiquinone) diradicals was proposed: Shultz, D. A.; Fico, R. M., Jr.; Bodnar, S. H.; Kumar, K.; Vostrikova, K. E.; Kampf, J. W.; Boyle, P. D. *J. Am. Chem. Soc.* **2003**, *125*, 11761−11771.

(18) Rajca, A.; Utamapanya, S. *J. Org. Chem.* **1992**, *57*, 1760−1767.

(19) Rassat, A.; Sieveking, U. *Angew. Chem., Int. Ed. Engl.* **1972**, *11*, 303−304.

(20) Rajca, A.; Rajca, S.; Desai, S. R.; Day, V. W. *J. Org. Chem.* **1997**, *62*, 6524−6528.

(21) Chiarelli, R.; Gambarelli, S.; Rassat, A. *Mol. Cryst. Liq. Cryst.* **1997**, *305*, 455−478.

(22) (a) Rozantsev, E. G. *Free Nitroxyl Radicals;* Plenum Press: New York, 1970; pp 135−139. (b) For the related nitroxide monoradicals, stability might be improved by replacement of the dimethylmethylene group at the nitroxide with a spirocyclohexyl group, though the evidence is not definitive.

(23) (a) Forrester, A. R.; Thompson, R. H. *Nature* **1964**, *203*, 74−75. (b) Calder, A.; Forrester, A. R. *J. Chem. Soc. C* **1969**, 1459−1464.

(24) The nonclassical C−H−O hydrogen bonds: (a) Taylor, R.; Kennard, O. *J. Am. Chem. Soc.* **1982**, *104*, 5063−5070. (b) Desiraju, G. R. *Acc. Chem. Res.* **1991**, *24*, 290−296.

(25) (a) Haldane, F. D. M. *Phys. Lett. A* **1983**, *93*, 464−468. (b) Haldane, F. D. M. *Phys. Rev. Lett.* **1983**, *50*, 1153−1156.

(26) Antiferromagnetic spin-1 chains of [Ni(1,3-diamino-2,2-dimethylpropane)$_2$-($\mu$-N$_3$)](PF$_6$): Tsujii, H.; Honda, Z.; Andraka, B.; Katsumata, K. *Phys. Rev. B* **2005**, *71*, 014426-1−6.

(27) Synthesis of [Ni(1,3-diamino-2,2-dimethylpropane)$_2$($\mu$-N$_3$)](PF$_6$): Monfort, M.; Ribas, J.; Solans, X.; Font-Bardía, M. *Inorg. Chem.* **1996**, *35*, 7633−7638.

(28) Zheludev, A.; Honda, Z.; Chen, Y.; Broholm, C. L.; Katsumata, K.; Shapiro, S. M. *Phys. Rev. Lett.* **2002**, *88*, 077206-1−4.

(29) Stone, M. B.; Zaliznyak, I. A.; Hong, T.; Broholm, C. L.; Reich, D. H. *Nature* **2006**, *440*, 187−190.

(30) Renard, J. P.; Verdaguer, M.; Regnault, L. P.; Erkelens, W. A. C.; Rossat-Mignod, J.; Stirling, W. G. *Europhys. Lett.* **1987**, *3*, 945−952.

(31) Anisotropy of Haldane gap in [Ni(1,3-diamino-2,2-dimethylpropane)$_2$($\mu$-N$_3$)](PF$_6$): Zheludev, A.; Chen, Y.; Broholm, C. L.; Honda, Z.; Katsumata, K. *Phys. Rev. B* **2001**, *63*, 104410-1−5.

(32) Spin-excitation spectrum in relatively more isotropic CsNiCl$_3$: Zaliznyak, I. A.; Lee, S. H.; Petrov, S. V. *Phys. Rev. Lett.* **2001**, *87*, 017202-1−4.

(33) 4,6-Diaminoisophthalate: Bogert, M. T.; Kropff, A. H. *J. Am. Chem. Soc.* **1909**, *31*, 841−848.

(34) Syntheses of benzobisoxazines by silica catalysis: Spagnol, G.; Rajca, A.; Rajca, S. *J. Org. Chem.* **2007**, *72*, 1867−1869.

**Scheme 1.** Synthesis of Nitroxide Diradicals **1**−**3**[a]
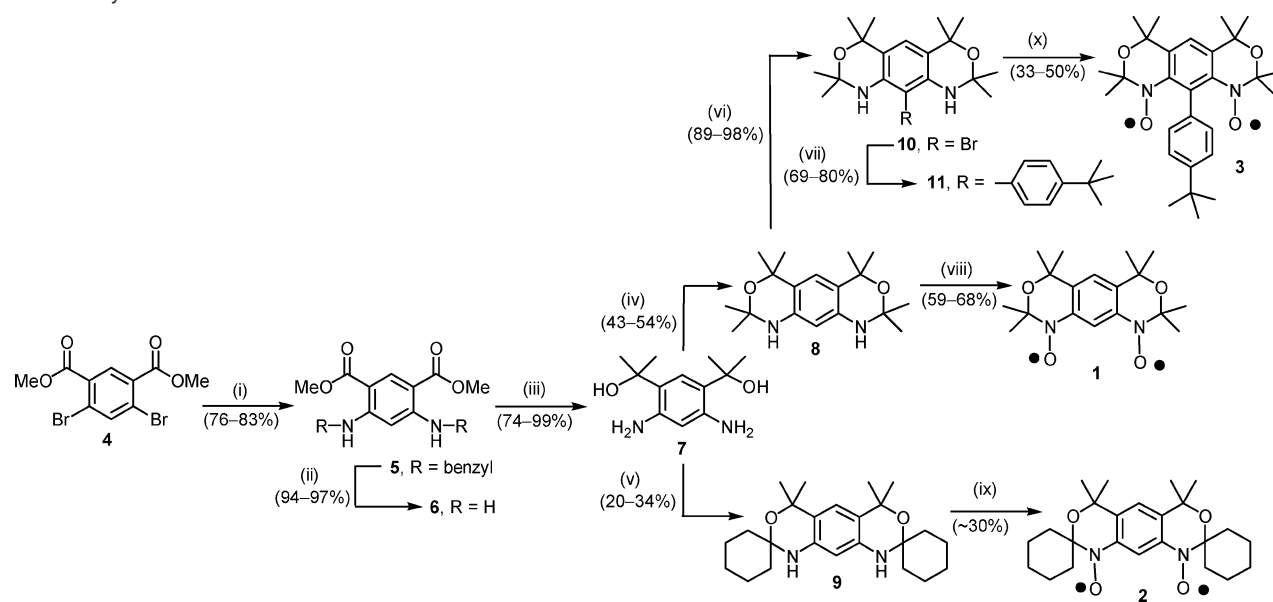


[a] Reagents and conditions: (i) Benzylamine (∼9 equiv), Pd(OAc)$_2$ (2.5 mol % per C−N bond), BINAP (3.8 mol % per C−N bond), toluene, ∼100 °C, 24−40 h; (ii) Pd/C (10 wt %, ∼5 mol %), ammonium formate (∼10 equiv), ethanol, reflux; (iii) CH$_3$MgBr (1.4 M in THF/toluene, 1:1, 14 equiv), THF, 0−25 °C, 11−24 h; (iv) acetone (∼100 equiv), acetic acid (2 equiv), pentane/benzene (∼2:1), 0 °C, 10 min, then reflux, ∼2 h; (v) cyclohexanone (∼80 equiv), acetic acid (∼0.4 equiv), benzene, reflux, 30 min; (vi) NBS (1.1 equiv), NaHCO$_3$ (12 equiv), Na$_2$SO$_4$ (12 equiv), chloroform, −40 °C, ∼1 h; (vii) 4-*tert*-butylphenylboronic acid (∼1.3 equiv), Pd(PPh$_3$)$_4$ (∼5 mol %), Na$_2$CO$_3$ (∼10 equiv), benzene/water/ethanol (2:2:1), 80 °C, ∼24 h; (viii) *m*CPBA (4 equiv), dichloromethane, 0 °C, ∼2 h; (ix) *m*CPBA (5 equiv), dichloromethane, 0 °C, ∼3 h; (x) *m*CPBA (4.5 equiv), dichloromethane, 0 °C, ∼2 h.

coupling of **10** with 4-*tert*-butylphenylboronic acid, adopting the conditions for bromoanilines,[35] provides diamine **11**.

Oxidation of tricyclic diamines **8**, **9**, and **11** using *m*CPBA (4+ equiv) provides the corresponding nitroxide diradicals **1**, **2**, and **3**, respectively. Careful optimization of both reaction conditions and purification methods improves the isolated yield of diradical **1** to ∼60%, compared to the previously reported yield of 10%.[19] The yield of ∼60% for **1** corresponds to a pure diradical, with diamagnetic and paramagnetic impurities at the level of <2%, as shown by ^{1}H NMR and electron paramagnetic resonance (EPR) spectroscopy, as well as magnetic studies. The isolated yields of diradicals **2** and **3** are 30−50%. However, diradical **2** is obtained with a significant amount of diamagnetic side products, but with a negligible content of paramagnetic impurities. Although the oxidation of sterically hindered diamine **11** with *m*CPBA yields relatively complex reaction mixtures, diradical **3** can be isolated as a pure compound after chromatographic separation at low temperature using deactivated silica gel.

The complexation of the conformationally constrained nitroxide diradicals with paramagnetic transition-metal ions was explored. Reaction of **1** with Mn(II)(hfac)$_2$ and Co(II)(hfac)$_2$ produces light brown crystals **12** and red crystals **13**, respectively (Figure 2).

The structures of **12** and **13** were determined by X-ray crystallography, which showed dimerization of the diradicals.

**Molecular Structures of Diradicals 1 and 3 and Dimers 12 and 13.** X-ray crystallographic data for diradicals **1** and **3** and dimers **12** and **13** are summarized in Table 1. Nitroxide diradical **1** crystallizes with one molecule per asymmetric unit, without inclusion of a solvent molecule.[36,37] The diradical
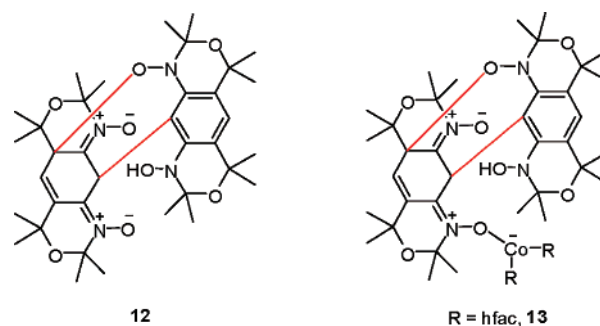


**Figure 2.** Dimers **12** and **13**. The C−O and C−C bonds connecting the two diradical frameworks are highlighted in red. Molecule of water complexed to the metal ion in **13** is not shown.

molecule has an approximate $C_2$ point group; the oxazine rings are in half-chair conformations, with the oxygen atoms (O3 and O4) on the opposite sides of the plane defined by the *m*-phenylene (Figure 3).[38]

In the structure of **3**, the diradical molecule has an approximate $C_s$ point group; the oxazine rings are in boatlike conformations, with the oxygen atoms (O3 and O4) on the same side of the plane defined by the *m*-phenylene (Figure 3). The 4-*tert*-butylphenyl group, which is disordered over two positions (Figure S1, Supporting Information), is severely twisted as indicated by the dihedral angles of 76.4(0.2)° and 73.4(0.7)° between its benzene ring plane and the N1-*m*-phenylene-N2 plane. The oxygens of the nitroxides (O1 and O2) are located

(35) Suzuki coupling of bromoanilines: Miura, Y.; Oka, H.; Momoki, M. *Synthesis* **1995**, 1419−1422.

(36) Crystal packing figure was shown for **1** and referred to as unpublished data in ref 21.

(37) (a) This crystal of **1** was obtained when **1** was crystallized in the presence of Cu(II)(hfac)$_2$ dihydrate. (b) Crystals with identical cell constants were obtained when **1** was crystallized from heptane/dichloromethane.

(38) 2,2-Dimethyl-1,4-dihydro-2*H*-3,1-benzoxazine shows a similar half-chair structure with the nitrogen atom coplanar with the benzene ring: Odabasoglu, M.; Özdamar, O.; Büyükgüngör, O. *Acta Crystallogr.* **2006**, *E62*, o908−o910.

***Table 1.*** Summary of the X-ray Crystallographic Data

| property | 1 | 3[a] | 12 (CH$_2$Cl$_2$)$_2$ | 13 (CH$_2$Cl$_2$)$_{0.75}$(CH$_3$COCH$_3$)$_{1.25}$ |
|---|---|---|---|---|
| molecular formula | C$_{18}$H$_{26}$N$_2$O$_4$ | C$_{28}$H$_{38}$N$_2$O$_4$ | C$_{38}$H$_{56}$Cl$_4$N$_4$O$_8$ | C$_{50.50}$H$_{65}$N$_4$O$_{13}$F$_{12}$Co |
| formula weight | 334.41 | 466.60 | 838.67 | 1296.17 |
| *T*, K | 130(2) | 95(2) | 130(2) | 130(2) |
| wavelength, Å | 0.71073 | 0.43321 | 0.71073 | 0.71073 |
| crystal/color | red block | red flat needle | light brown block | red block |
| crystal system | monoclinic | orthorhombic | monoclinic | triclinic |
| space group | *P*2$_1$/*c* | Pbca | *C*2 | *P*1̄ |
| *a*, Å | 8.7862(9) | 8.658(5) | 25.4534(11) | 12.0460(17) |
| *b*, Å | 8.0998(8) | 20.436(11) | 12.5714(6) | 14.3395(19) |
| *c*, Å | 24.100(2) | 28.965(17) | 17.3570(8) | 18.279(3) |
| α, deg | 90 | 90 | 90 | 85.068(3) |
| β, deg | 92.679(3) | 90 | 131.3080(10) | 87.920(3) |
| γ, deg | 90 | 90 | 90 | 68.748(3) |
| *V*, Å$^3$ | 1713.2(3) | 5125(5) | 4172.0(3) | 2931.8(7) |
| Z | 4 | 8 | 4 | 2 |
| *D*$_{calcd}$/g cm$^{-3}$ | 1.297 | 1.209 | 1.335 | 1.468 |
| abs coeff/mm$^{-1}$ | 0.092 | 0.051 | 0.338 | 0.464 |
| reflns collected | 23186 | 25457 | 29506 | 35042 |
| reflns obsd (*I* > 2σ(*I*)) | 2880 | 2238 | 7901 | 8759 |
| data/restraints/params | 3489/0/251 | 4586/72/347 | 8583/16/513 | 12008/95/810 |
| R1 (*I* > 2σ(*I*))/R1 (all data) | 0.0368/0.0922 | 0.1178/0.1937 | 0.0570/0.0625 | 0.0517/0.0789 |
| wR2 (*I* > 2σ(*I*))/wR2 (all data) | 0.0922/0.1031 | 0.2739/0.3285 | 0.1617/0.1699 | 0.1311/0.1502 |
| absolute structure param[b] | | | -0.02(7) | |
| GOF | 1.030 | 0.993 | 1.056 | 1.022 |

[a] This structure has a relatively lower quality, as the crystals were very small and they decayed under synchrotron radiation. [b] The Flack parameter is well determined with chlorine anomalous dispersion.

on the same side of the N1-*m*-phenylene-N2 plane, while the 4-*tert*-butylphenyl group is located on the other side with an angle of −14.51° between the C19C10 bond axis and the N1-*m*-phenylene-N2 plane. These out-of-plane distortions may reflect the steric congestion of the nitroxides with the 4-*tert*-butylphenyl group.

Concerning magnetic properties of **1** and **3**, the degree of coplanarity for the nitroxide-*m*-phenylene-nitroxide exchange coupling pathway is the most important factor. In **1**, the mean deviations from calculated least-squares planes including the *m*-phenylene and the nitroxides, as well as the angles between the ON bond axes of the nitroxides with the N1-*m*-phenylene-N2 plane, are negligibly small.[39,40] Therefore, the nitroxides are coplanar with the *m*-phenylene, forming an exchange coupling pathway for a strong ferromagnetic coupling. In **3**, the corresponding mean deviations and angles are significantly larger than those in **1**, indicating that the nitroxides are moderately distorted from coplanarity with *m*-phenylene.[40,41] Thus, the exchange coupling in **3** should still be ferromagnetic but somewhat weaker that that in **1**.[15,16]

In diradicals with planar conformation such as that in **1**, efficient delocalization of spin density from the two nitroxides into the *m*-phenylene is expected. Consequently, the presence of large spin density at the ortho/ortho (C10) and para/ortho (C4 and C6) positions is anticipated. Such large spin density

may promote dimerization at these positions, as observed for **12** and **13**. Evidence of extensive delocalization of spin density into the *m*-phenylene in **1** is found by $^1$H NMR and EPR spectroscopy. The presence of large spin densities at the ortho/ortho position in **1** and **3** is supported by DFT calculations.

Fully optimized geometries for the lowest triplet states of **1** and **3** at the UB3LYP/6-31G* level are similar to those obtained from the X-ray structures.[42,43] A large fraction of spin density is delocalized to *m*-phenylene; the delocalization into the severely twisted 4-*tert*-butylphenyl group in **3** is rather small (Figure 4). For example, the spin densities of +0.28 and +0.24 at the ortho/ortho position (C10) are calculated in **1** and **3**, respectively. This also suggests that the spin delocalization is somewhat larger in **1**,[44] which may correspond to the larger singlet triplet energy gap at the UB3LYP/6-31G* level, that is, 2*J*/*k* = +1600 K (3.3 kcal/mol) for **1** and 2*J*/*k* = +1100 K (2.2 kcal/mol) for **3**.[45] Both energy gaps are significantly greater than the thermal energy at room temperature.

**Structure of Diradicals 1, 2, and 3 in Solution. (i) $^1$H NMR Spectroscopy.** $^1$H NMR spectra of diradicals **1**, **2**, and **3** in acetone-*d*$_6$ at room temperature show resonances for those protons that are expected to possess relatively small spin densities (i.e., all protons except those of the *m*-phenylene moieties of the dinitroxides).[46,47] The paramagnetic shifts (Δδ$_p$ in ppm) for the observed $^1$H resonances in the diradicals were

(39) In diradical **1**, the mean deviations from a calculated least-squares plane including nitroxides and *m*-phenylene are 0.0052 and 0.0223 Å for N1-*m*-phenylene-N2 plane and O1N1-*m*-phenylene-N2O2 plane, respectively. The angles of the O1N1 and O2N2 bond axes with the N1-*m*-phenylene-N2 plane are 1.68° and 3.89°, respectively.

(40) In **1** and **3**, the nitroxide moieties are planar, as measured by the sums on bond angles around N1 and N2 (Table S1, Supporting Information).

(41) In diradical **3**, the mean deviations from calculated least-squares planes including nitroxides and *m*-phenylene are 0.0265 and 0.1881 Å for N1-*m*-phenylene-N2 plane and O1N1-*m*-phenylene-N2O2 plane, respectively. The angles of the O1N1 and O2N2 bond axes with the N1-*m*-phenylene-N2 plane are 29.86° and 29.20°, respectively.

(42) Frisch, M. J.; et al. *Gaussian 03*; Gaussian, Inc.: Wallingford, CT, 2004.

(43) The full geometry optimization of **3** (triplet state) at the UB3LYP/6-31G* level, using the same starting conformation for the benzobisoxazine moiety as that in **1**, gives a conformation with partially converged geometry, in which the oxygens of the nitroxides are on the opposite sides of the *m*-phenylene plane (Supporting Information). This conformation is 1.3 kcal mol$^{-1}$ above the lowest triplet-state conformation for **3**.

(44) The spin densities (+0.51) for the oxygens of the distorted nitroxides in the lowest triplet state of **3** are larger than the spin densities (+0.49) for the oxygens of the planar nitroxides in the triplet state of **1**.

(45) The UB3LYP (broken symmetry) level of theory usually overestimates the singlet−triplet gaps in organic diradicals.
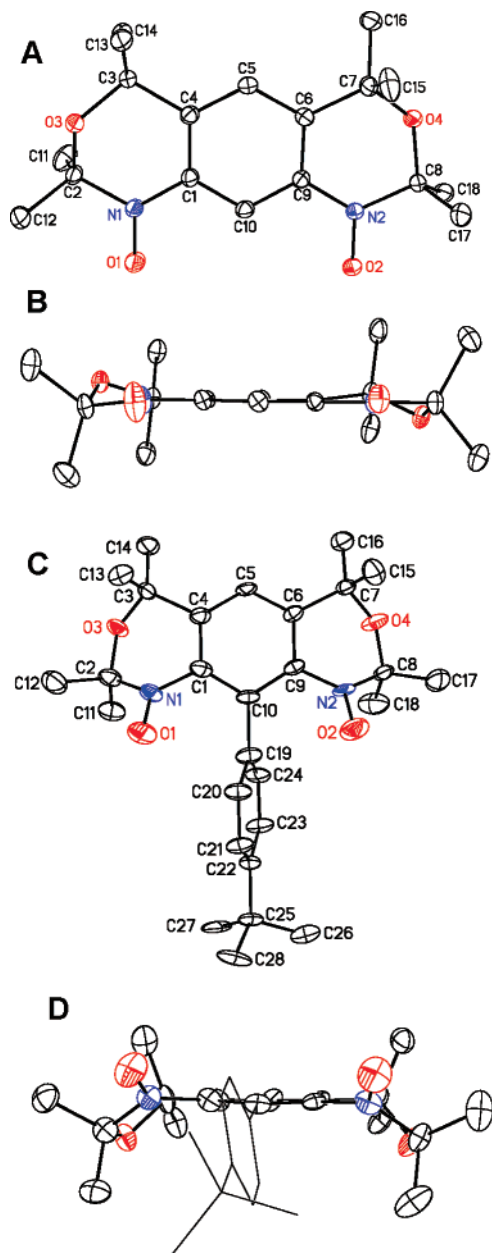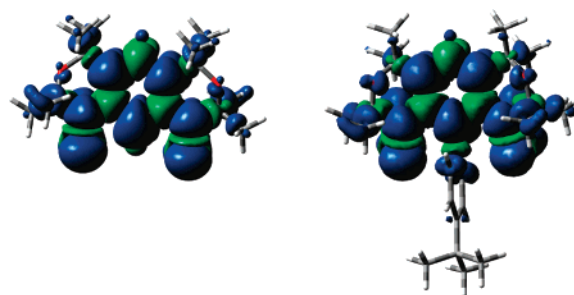
**Figure 4.** UB3LYP/6-31G* spin densities for the triplet-state nitroxide diradicals **1** (left) and **3** (right). The blue and green lobes correspond to positive and negative densities, respectively.

***Table 2.*** Summary of ¹H NMR (Acetone-$d_6$) Chemical Shifts ($\delta$), Paramagnetic Shifts ($\Delta\delta_p$), and ¹H-Hyperfine Splittings ($a_H$) for Diradicals **1** and **3**[a]

| | $\delta$ (ppm) | | $\Delta\delta_p$ (ppm) | | $a_H$ (mT) | |
|---|---|---|---|---|---|---|
| | **1** | **3** | **1** | **3** | **1** | **3** |
| C11, 12, 17, 18 | −0.33 | +8.1 | −2.4 | +6.0 | −0.002 | +0.006 |
| C13, 14, 15, 16 | +24.8 | +24.2 | +22.7 | +22.1 | +0.023 | +0.022 |
| C20, 24 | | −10.5 | | −18.6 | | −0.019 |
| C21, 23 | | +21.1 | | +13.0 | | +0.013 |
| C22 | | | | | | |
| C26, 27, 28 | | +1.68 | | −0.4[b] | | −0.0004[b] |

[a] Atom numbering scheme is based upon X-ray structures for **1** and **3**, as shown in Figure 3 and in the Supporting Information (CIFs). [b] The values of $\Delta\delta_p$ and $a_H$ for the *tert*-butyl protons may be viewed as negligible.

(Figure 5). The less broadened singlet at −0.33 ppm is assigned to the protons of the dimethylmethylenes directly connected to the nitroxides. The negative paramagnetic shift, $\Delta\delta_p \approx −2.4$ ppm, corresponds to a negative value of $a_H = −0.002$ mT (−0.02 G). This is consistent with the presence of a very small negative spin density at these hydrogens, as predicted by the spin polarization mechanism.

The singlet at 24.8 ppm is assigned to the protons of the dimethylmethylene groups in the ortho/para positions with respect to the nitroxides. The positive paramagnetic shift, $\Delta\delta_p = +22.7$ ppm, corresponds to the positive value of $a_H = +0.023$ mT (+0.23 G). Thus, a relatively large and positive spin density is found on these 12 hydrogen atoms. This is consistent with the conjugative mechanism ("homohyperconjugation")[49] for the transfer of positive spin density from ortho/para positions to the methyl hydrogens, as observed for 4-alkylphenyl-*tert*-butylnitroxide radicals, *tert*-butyl-substituted phenoxy radicals, and *tert*-butyl-substituted polyarylmethyl polyradicals.[50−52] However, the value of $a_H = +0.023$ mT is significantly greater than

(48) (a) McConnell, H. M.; Chesnut, D. B. *J. Chem. Phys.* **1958**, *28*, 107−117. (b) Chakravorty, A.; Holm, R. H. *Inorg. Chem.* **1964**, *3*, 1010−1015. (c) For a diradical in the high-spin state with the value of total spin *S*, paramagnetic contact shift $\Delta\delta_p$ (in ppm) for ¹H may be expressed as $\Delta\delta_p = −a_H(\gamma_e/\gamma_H)[g\mu_B S(S + 1)/6SkT]10^6$, where $\gamma_e$ and $\gamma_H$ are gyromagnetic ratios for electrons and protons, respectively, and the other symbols have their usual meaning.
(49) Homohyperconjugation: (a) Russell, G. A.; Chang, K. Y. *J. Am. Chem. Soc.* **1965**, *87*, 4381−4383. (b) Russell, G. A.; Holland, G.; Chang, K. Y.; Zalkow, L. H. *Tetrahedron Lett.* **1967**, *21*, 1955−1959.
(50) ¹H NMR spectra of 4-alkylphenyl-*tert*-butylnitroxide radicals: (a) Torsell, K.; Goldman, J.; Petersen, T. E. *Liebigs Ann. Chem.* **1973**, 231−240. (b) The reported values of $a_H$ (mT) for the protons of the methyl groups were: $a_H = +0.0054$ (*t*-Bu), $a_H = +0.0055$ (*i*-Pr), and $a_H = +0.0117$ (Et).
(51) ¹H NMR spectra of *tert*-butyl-substituted phenoxy radicals: (a) Kreilick, R. W. *Mol. Phys.* **1968**, *14*, 495−499. (b) Paramagnetic shifts (versus the diamagnetic phenol precursor) and values of $a_H$ (mT): for 2,4,6-tri-*tert*-butylphenoxy radical, 4-*t*-Bu, +28.6 ppm ($a_H = +0.0385$); 2-*t*-Bu and 6-*t*-Bu, +5.4 ppm ($a_H = +0.0073$); 4-(4′-*tert*-butylphenylene)-2,6-di-*tert*-butylphenoxy radical, *o*-Ph, −132.5 ppm ($a_H = −0.179$); *m*-Ph, +50 ppm ($a_H = +0.067$); *t*-Bu-*p*-Ph, +5.1 ($a_H = +0.0069$).

**A**

**B**

**C**

**D**

**Figure 3.** Molecular structure and conformation for nitroxide diradicals **1** and **3**: (A) top view of **1**, (B) side view of **1**, (C) top view of **3**, (D) side view of **3**. In the top views, carbon, nitrogen, and oxygens atoms are depicted with thermal ellipsoids set at the 50% probability level. Hydrogen atoms and disorder (in **3**) are omitted for clarity.

determined with reference to the corresponding diamagnetic diamines, after a relatively small correction for the bulk paramagnetic susceptibility shift (e.g., ∼0.7 ppm downfield shift for an ∼0.05 M solution of **1** or **3**). Using the values of $\Delta\delta_p$, both magnitude and sign of isotropic electron−proton hyperfine splittings ($a_H$ in mT) for an $S = 1$ diradical at room temperature (295−298 K) may be estimated using eq 1 (Table 2).[48]

$$a_H = 0.0010\ \Delta\delta_p \qquad (1)$$

A solution of 0.05 M diradical **1** in acetone-$d_6$ shows two broad singlets at +24.8 and −0.33 ppm, with 1:1 integration

(46) *NMR of Paramagnetic Molecules*; La Mar, G. N., Horrocks, W. DeW., Jr., Holm, R. H., Eds.; Academic: New York, 1973.
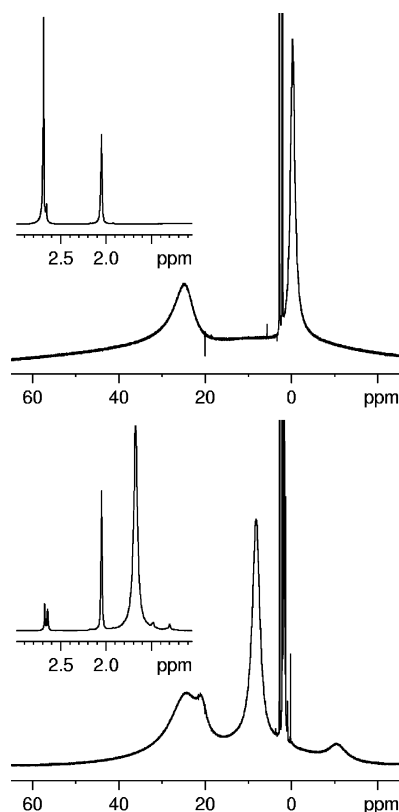(47) Sharp, R. R. *Nucl. Magn. Reson.* **2005**, *34*, 553−596.

**Figure 5.** $^1$H NMR (500 MHz, acetone-$d_6$, LB = 0.3 Hz) spectra for ∼46 mM diradical **1** (top) and ∼49 mM diradical **3** (bottom). Three sharp peaks (insets) at 2.050 and 2.6−2.7 ppm correspond to the residual, partially deuterated acetone, $H_2O$, and HDO.



**Figure 6.** EPR (X-band) spectra for ∼1 mM diradicals **1** and **3** in EtOH at 133−134 K. (A) Expansion of the $|\Delta m_s| = 1$ transitions near the *y*-turning point and simulation at 134 K for **1**. (B) $|\Delta m_s| = 1$ transitions and simulation at 134 K for **1**. (C) $|\Delta m_s| = 2$ transition at 134 K for **1**. (D) $|\Delta m_s| = 1$ transitions and simulation at 133 K for **3**. (E) $|\Delta m_s| = 2$ transition at 133 K for **3**. Key parameters for the spectral simulations of the $S = 1$ states are reported in Table 3. Gaussian line widths are $L_x = 0.78$, $L_y = 0.42$, $L_z = 0.82$ mT for **1**, and $L_x = 1.9$, $L_y = 0.67$, $L_z = 1.2$ mT for **3**.

the corresponding values of $a_H$ in 4-alkylphenyl-*tert*-butylnitroxide radicals,[50] suggesting a relatively large spin density at the ortho/para positions.[53] This indicates significant delocalization of spin density into the *m*-phenylene in **1**.

A solution of 0.05 M diradical **3** in acetone-$d_6$ shows five broad singlets (Figure 5). Two 12-proton singlets at 24.2 and 8.1 ppm are assigned to the protons of the dimethylmethylene groups, in the ortho/para positions and in the proximate positions with respect to the nitroxides, respectively. The other three singlets are assigned to the protons of the 4-*tert*-butylphenyl group: 21.1 ppm (2H, meta), 1.7 (9H, *t*-Bu), −10.5 (2H, ortho).

The paramagnetic shift (Table 2), corresponding to the singlet at 24.2 ppm, suggests that the delocalization of spin density into the *m*-phenylene in **3** is slightly less than that in **1**. The positive paramagnetic shift for the protons of the dimethylmethylene groups within proximity to the nitroxides suggests that the conjugative mechanism becomes more important than the spin polarization mechanism, perhaps because of different conformation of the oxazine rings and the nitroxides in **3**, compared to that in **1**.
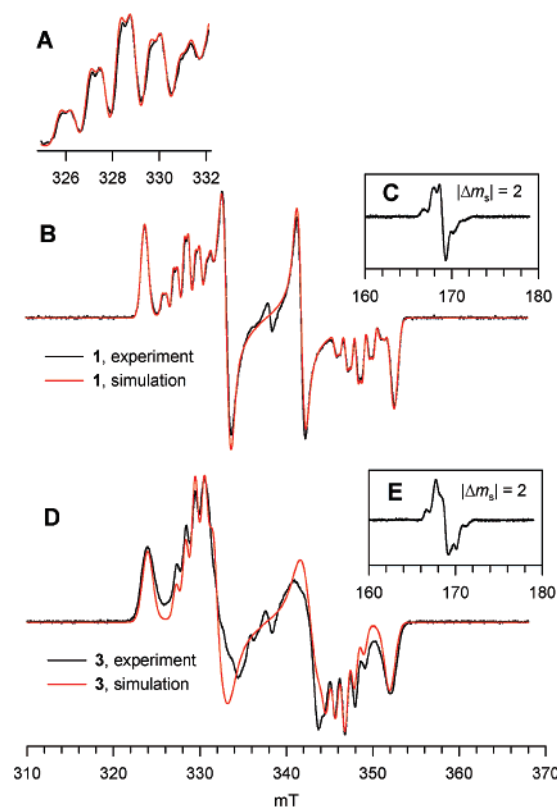
The paramagnetic shifts for the ortho and meta protons of the severely twisted 4-*tert*-butylphenyl group give $a_H = −0.019$ mT and $a_H = +0.013$ mT, respectively (Table 2); that is, $|a_H|$ for the ortho protons is rather small and becomes similar to $|a_H|$ for the meta protons, indicating minimal delocalization of spin density into the benzene ring in **3**.[54,55] Similarly to the biphen-4-yl-*tert*-butylnitroxide radical,[54] the negative and positive signs of $a_H$ for the ortho and the meta protons are consistent with the positive and negative π-spin density at the ortho and the meta carbons. The paramagnetic shift for the *tert*-butyl protons is negligible, not suitable for reliable determination of its sign.

**(ii) EPR Spectroscopy.** The EPR spectra of 1 mM nitroxide diradical **1** in EtOH at 140 K are similar to that reported by Rassat and Sieveking (Table 3 and Figure S4, Supporting Information).[19] Analogous spectra are obtained for **1** and **2** in 2-methyltetrahydrofuran (2-MeTHF), including the observation

(52) $^1$H NMR spectrum of polyarylmethyl triradical: (a) Rajca, S.; Rajca, A. *J. Am. Chem. Soc.* **1995**, *117*, 9172−9179. (b) The $^1$H resonance at +10 ppm was assigned to *t*-Bu groups in 4-*tert*-butylphenyls adjacent to the radicals; the sign of the spin density at the hydrogens of the *t*-Bu group should be re-assigned as positive.

(53) (a) The conjugative mechanism ("homohyperconjugation") for transfer of spin density is most effective when the $2p_\pi$ orbital at the ortho/para position is coplanar with the C−C(Me) bond of the dimethylenemethylene group. (b) Underwood, G. R.; Vogel, V. L. *J. Am. Chem. Soc.* **1971**, *93*, 1058−1063. (c) Reference 46. (d) Selected torsional angles, involving dimethylmethylene group in **1**: C14−C3−C4−C5 = −52.05(16)°, C13−C3−C4−C5 = 69.69(15)°, C5−C6−C7−C16 = −45.21(17)°, C5−C6−C7−C15 = 77.64(15)°.

(54) $^1$H NMR spectrum of biphen-4-yl-*tert*-butylnitroxide radical: (a) Forrester, A. R.; Hepburn, S. P.; McConnachie, G. *J. Chem. Soc., Perkin Trans. 1* **1974**, 2213−2219. (b) The chemical shifts and values of $a_H$ (mT) for protons in the 4-phenyl ring and the *tert*-butyl group were as follows: *m′*-H, +16 ppm ($a_H = +0.012$), *o′,p′*-H, -13 ppm ($a_H = −0.028$), *t*-Bu, −4 ppm ($a_H = −0.007$).

(55) For arylnitroxides, in which the aryl ring and nitroxide moiety are expected to be nearly perpendicular, such as in 2-methylphenyl-*tert*-butylnitroxide radical and 2,6-dimethylphenyl-*tert*-butylnitroxide radical, values $|a_H|$ for the para, ortho, and meta protons are nearly identical: Calder, A.; Forrester, A. R.; Emsley, J. W.; Luckhurst, G. R.; Storey, R. A. *Mol. Phys.* **1970**, *18*, 481−489.

***Table 3.*** EPR Spectral Parameters for Diradicals **1**, **2**, and **3**[a]

| | solvent | $T$ (K) | $\nu$ (GHz) | $g_x$ | $g_y$ | $g_z$ | $|D/hc|/10^{-4}$ (cm$^{-1}$) | $|E/hc|/10^{-4}$ (cm$^{-1}$) | $|A_{yy}/2hc|/10^{-4}$ ($^{14}$N, cm$^{-1}$) | $|A_{yy}/hc|/10^{-4}$ ($^1$H, cm$^{-1}$) |
|---|---|---|---|---|---|---|---|---|---|---|
| **1** | EtOH | 134 | 9.4907 | 2.0086 | 2.0022 | 2.0052 | 135.0 | 17.5 | 11.9 | 4.4 |
| | | 140 | 9.4868 | 2.0086 | 2.0022 | 2.0050 | 133.8 | 16.8 | 11.9 | |
| | 2-MeTHF | 140 | 9.6504 | 2.0084 | 2.0024 | 2.0052 | 130 | 15.5 | 11.5 | |
| **2** | 2-MeTHF | 140 | 9.6511 | 2.0084 | 2.0024 | 2.0052 | 131.5 | 16 | 11.5 | |
| **3** | EtOH | 133 | 9.4839 | 2.0078 | 2.0037 | 2.0050 | 131.0 | 10.0 | 10.2 | |

[a] Microwave frequencies ($\nu$) are dependent on the cavity type and the sample.

of the $|\Delta m_s| = 2$ transition (Table 3, Figures S5 and S6, Supporting Information).

The spectra for diradical **1** in EtOH are better resolved at lower temperatures (Figure 6, Table 3). In the $|\Delta m_s| = 1$ region at 134 K, three nearly symmetrically disposed pairs of peaks, characteristic of an $S = 1$ state with a significant value of zero-field splitting (zfs) parameter $|E/hc|$, are observed for **1**. The values of the zfs parameters obtained from spectral simulations (Figure 5) are $|D/hc| = 1.350 \times 10^{-2}$ cm$^{-1}$ ($|D/g\mu_B| = 14.45$ mT) and $|E/hc| = 1.75 \times 10^{-3}$ cm$^{-1}$ ($|E/g\mu_B| = 1.87$ mT). The middle pair of peaks consists of symmetrical pentuplets, corresponding to the $^{14}$N hyperfine coupling with spacings of $|A_{yy}/2hc| = 0.00119$ cm$^{-1}$ ($|A_{yy}/2g\mu_B| = 1.27$ mT) from two nitrogen atoms. Each peak of the pentuplet is broadened with the doublet-like pattern, which corresponds to a relatively smaller spacing of ~0.5 mT (Figure 5, expanded plot). This additional splitting is assigned to the $^1$H hyperfine coupling with spacings of $|A_{yy}/hc| = 0.00044$ cm$^{-1}$ ($|A_{yy}/g\mu_B| = 0.48$ mT) because of one hydrogen atom at the ortho/ortho position. Because the largest principal value $^{14}$N hyperfine tensor in nitroxide radicals coincides with the direction of the nitrogen $2p_\pi$ orbital,[56] the well-resolved $^{14}$N hyperfine coupling implies that the $2p_\pi$ orbital is approximately parallel to the $y$-axis, which is the direction of the second largest principal value of the magnetic dipole tensor.[57] Therefore, the nitroxides and $m$-phenylene in diradical **1** adopt a coplanar conformation. In the coplanar conformation, the spin density is likely to be significantly delocalized from the nitroxide moieties onto the $m$-phenylene. This delocalization should lead to the relatively lower value of $^{14}$N hyperfine coupling, as illustrated by the largest principal values of the $^{14}$N hyperfine tensor for "planarized" diradical **1** (0.0024 cm$^{-1}$), *tert*-butylarylnitroxide diradical (0.0026 cm$^{-1}$),[57] and localized di-*tert*-butylnitroxide radical (0.0030 cm$^{-1}$).[56] Additional evidence for the spin delocalization in **1** is provided by the large value of $|A_{yy}/g\mu_B| = 0.48$ mT for the $^1$H hyperfine coupling for the hydrogen at the ortho/ortho position. The $|A_{yy}/g\mu_B|$ corresponds to the orientation of the magnetic field parallel to the carbon $2p_\pi$ orbital and perpendicular to the C(sp$^2$)−H bond axis, and it should be approximately equal to the value of isotropic $^1$H splitting ($a_H$).[58,59] Notably, the value of $|a_H| \approx 0.48$ mT in diradical **1** is approximately ***two times greater***, compared to the values of $a_H$ for ortho hydrogens in conformationally unrestricted alkylphenyl nitroxide radicals.[50,60] This implies the presence of a relatively large spin density at the ortho/ortho position (C10) of the

$m$-phenylene, which is consistent with the finding of relatively large spin density at the ortho/para positions (C4 and C6) by $^1$H NMR spectroscopy. Because the strength of the ferromagnetic exchange coupling through $m$-phenylene may be empirically related through values of $|a_H|$ to the square of the spin density residing in the $m$-phenylene,[1b] planar diradicals **1** and **2** are expected to possess very strong ferromagnetic coupling, compared to conformationally unrestricted $m$-phenylene-based nitroxide diradicals.

EPR spectra for diradical **3** in EtOH at 133 K are qualitatively similar to those for **1** (Figures 6 and S7, Supporting Information). The value of $|D/hc| = 1.31 \times 10^{-2}$ cm$^{-1}$ ($|D/g\mu_B| = 14.0$ mT), which is primarily determined by the inter-radical distance, is nearly identical to that in **1**. The relatively smaller value of $|E/hc| = 1.00 \times 10^{-3}$ cm$^{-1}$ ($|E/g\mu_B| = 1.07$ mT) may be associated with the distortion from planarity in **3**.[1f] Another indication for a nonplanar structure of **3** is provided by the line broadening for the inner and outer pairs of peaks, most likely due to the increased, but unresolved, $^{14}$N hyperfine coupling along the directions of the smallest ($x$-axis) and the largest ($z$-axis) principal values of the magnetic dipole tensor. The middle pair of the peaks still appears as a partially resolved pentuplet but with the splitting $|A_{yy}/2hc| = 0.00102$ cm$^{-1}$ ($|A_{yy}/2g\mu_B| = 1.09$ mT), which is significantly smaller than that in **1**. This indicates that the largest principal value of the $^{14}$N hyperfine tensor, which coincides with the direction of the nitrogen $2p_\pi$ orbital,[56] is not parallel to any of the directions of the principal values of the magnetic dipole tensor ($x$-, $y$-, or $z$-axes). This is consistent with the X-ray structure of **3**, in which the oxygen atoms (O1 and O2) with large spin density are bent out of the N1-$m$-phenylene-N2 plane.

Stability of nitroxide diradicals **1** and **3** at millimolar concentrations in degassed EtOH or EtOH/dichloromethane is studied by EPR spectroscopy (Figures S7−S11, Supporting Information). EPR spectra for samples of **1**, for which neither diamagnetic nor $S = 1/2$ paramagnetic impurities are detectable ($^1$H NMR and EPR spectroscopy), were unchanged after 2 days at room temperature. This is in contrast to the report by Rassat and Sieveking that **1** slowly decomposes in solution.[19] Perhaps purity of **1** may be crucial for its stability in solution. EPR spectra for solutions of **3** in EtOH, which were kept for 2 and 4 days at room temperature, show progressive growth of the center lines, which are assigned to the $S = 1/2$ paramagnetic impurities, though the $S = 1$ diradical remains the predominant paramagnetic species. Considering that the nitroxides and the $m$-phenylene are sterically shielded to greater extent in **3**, compared to those in **1**, it is surprising that **3** decomposes (although very slowly) in solution.

(56) Griffith, O. H.; Cornell, D. W.; McConnell, H. M. *J. Chem. Phys.* **1965**, *43*, 2909−2910.

(57) Rajca, A.; Mukherjee, S.; Pink, M.; Rajca, S. *J. Am. Chem. Soc.* **2006**, *118*, 13497−13507.

(58) McConnell, H. M.; Heller, C.; Cole, T.; Fessenden, R. W. *J. Am. Chem. Soc.* **1960**, *82*, 766−775.

(59) Morton, J. R. *Chem. Rev.* **1964**, *64*, 453−471.

(60) Isotropic $^1$H splitting, $a_H = 0.35$ mT, assigned to the hydrogen at the ortho/ortho position, for **1** in "solutions of low viscosity" was reported in ref 19.
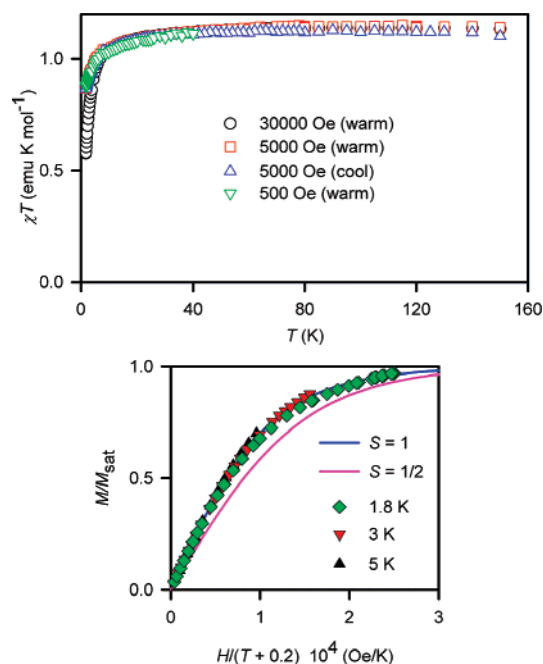
**Figure 7.** SQUID magnetometry for ∼5 mM diradical **1** in THF. Top: $\chi T$ vs $T$ plots in both cooling and warming modes, with $\chi T \approx 1.1$ emu K mol$^{-1}$ in the high-temperature range. Bottom: $M/M_{sat}$ vs $H/(T - \theta)$ plots, with solid lines showing plots of Brillouin functions with $S = \frac{1}{2}$ and $S = 1$; numerical fits to the Brillouin functions with $\theta = -0.2$ K give $S = 0.91$ and $M_{sat} \approx 1.1$ $\mu_B$ at 1.8, 3, and 5 K.



**Figure 8.** SQUID magnetometry for ∼15 mM diradical **3** in THF. Top: $\chi T$ vs $T$ plots in both cooling and warming modes, with $\chi T = 0.87$ emu K mol$^{-1}$ in the high-temperature range. Bottom: $M/M_{sat}$ vs $H/(T - \theta)$ plot, with solid lines showing plots of Brillouin functions with $S = \frac{1}{2}$ and $S = 1$; numerical fits to the Brillouin functions with $\theta = -0.085 \approx -0.1$ K give $S = 0.98$ and $M_{sat} = 0.87$ $\mu_B$ at 1.8, 3, and 5 K.

**Magnetic Studies of 1, 2, and 3 in Solution.** Magnetization ($M$) is measured as a function of magnetic field ($H = 0-5 \times 10^4$ Oe and $T = 1.8, 3,$ and 5 K) and temperature ($T = 1.8-150$ K at $H = 30\,000$, 5000, or 500 Oe) for **1**, **2**, and **3** in tetrahydrofuran (THF). The $M$ vs $H$ and $M$ vs $T$ data are plotted as the $M/M_{sat}$ vs $H/T$ and the $\chi T$ vs $T$, respectively, where $M_{sat}$ is the magnetization at saturation and $\chi$ is the paramagnetic susceptibility.

The magnetization ($M$) vs magnetic field ($H$) data at low temperatures ($T = 1.8, 3, 5$ K) provide good fits to the Brillouin functions with a mean-field parameter ($\theta < 0$), that is, $M$ vs $H/(T - \theta)$. The fits have two variable parameters, that is, total spin ($S$) and magnetization at saturation ($M_{sat}$); the mean-field parameter $\theta$ is adjusted until the $M/M_{sat}$ vs $H/(T - \theta)$ plots overlap at all temperatures. For **1**, **2**, and **3**, the values of $S \approx 1$ (0.91–0.99), determined from the curvature of the Brillouin plots, indicate the triplet ($S = 1$) ground states (Figures 7, 8, and S12–S14, Supporting Information). Because the values of $\theta < 0$ are rather small ($|\theta| < 0.5$ K), it is almost certain that they correspond to intermolecular antiferromagnetic coupling.

Magnetization at saturation ($M_{sat}$) measures the number of unpaired electron spins (or spin concentration) at the limit of low temperature and high magnetic field. For a diradical, $M_{sat}$ should be 1.00 in units of Bohr magnetons ($\mu_B$) per radical site, as long as strong antiferromagnetic exchange coupling ($|\theta| > 1$ K) is absent. The measured values of $M_{sat}$ for **1**, **2**, and **3** are 1.0 (averaged for three samples), 0.65, and 0.87 $\mu_B$, respectively. Unlike the values of $S$, the values of $M_{sat}$ are dependent upon the mass of the diradical. Therefore, values of $M_{sat}$ would be underestimated if mass transfers of small amounts (0.1–1 mg) of electrostatic powders of diradicals are incomplete during the preparation of the samples for SQUID magnetometry. For the most dilute solutions of diradicals, which required ∼0.1 mg of
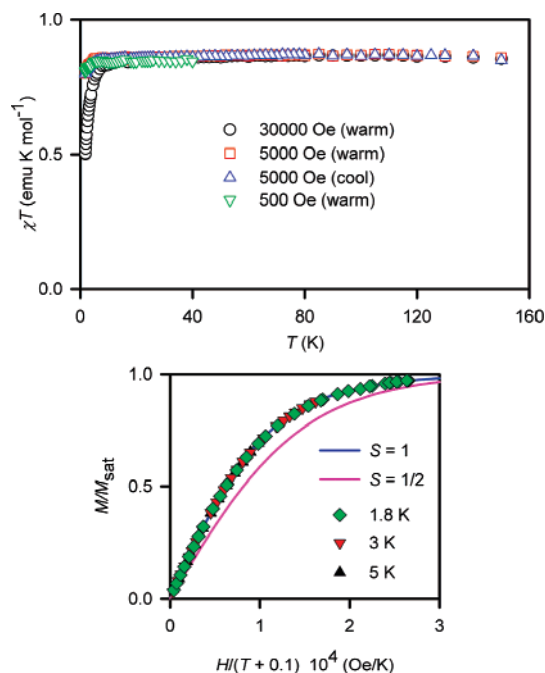
diradical, weighing errors may become significant, leading to either increased or decreased value of $M_{sat}$.

The value of $\chi T$ (product of magnetic susceptibility and temperature) and its temperature dependence measure both the ground state and the strength of exchange coupling in diradicals **1**–**3** (Figures 7 and 8). For an $S = 1$ diradical with strong ferromagnetic coupling, the value of $\chi T$ should be 1.00 emu K mol$^{-1}$ (per mole of diradical). The measured values of $\chi T$ (in units of emu K mol$^{-1}$) are nearly identical to the numerical values of $M_{sat}$ (in the unit of $\mu_B$) for each sample of diradical (Table 1). Therefore, $\chi T \approx 1$ is found for all samples of diradicals **1**, **2**, and **3**, after the values of $\chi T$ are corrected for spin concentration ($M_{sat}$). Although the $\chi T$ vs $T$ plots are nearly flat, small errors in the correction for diamagnetism may have a significant impact on such plots, especially at higher temperatures. Therefore, only a lower limit of more than $2J/k > 200$ K (0.4 kcal mol$^{-1}$) for the singlet–triplet energy gap may be estimated for **1**, **2**, and **3** in THF. This is consistent with strong ferromagnetic coupling. A better estimate for the singlet–triplet energy gap, and thus the strength of the exchange coupling, is obtained from magnetic studies of diradicals in the solid state, using an accurate point-by-point correction for diamagnetism and a wider temperature range (up to 290 K).

**Magnetic Studies of Diradicals 1–3 in the Solid State. (i) Singlet–Triplet Gaps.** For polycrystalline **1**, the $\chi T$ vs $T$ plot shows a downward turn from the $S = 1$ paramagnetic value of $\chi T \approx 0.99$ emu K mol$^{-1}$ at room temperature to $\chi T \approx 0.12$ emu K mol$^{-1}$ at 1.8 K (Figures 9 and S15, Supporting Information). For polycrystalline **2**, similar $\chi T$ vs $T$ plots are found; $\chi T$ is constant at $T \approx 100-290$ K, though $\chi T \approx 0.8$ emu K mol$^{-1}$ at room temperature is lower than the expected value of 1.00 emu K mol$^{-1}$ for $S = 1$ diradical. Because the downward curvature of the $\chi T$ versus $T$ plot for **2** is much
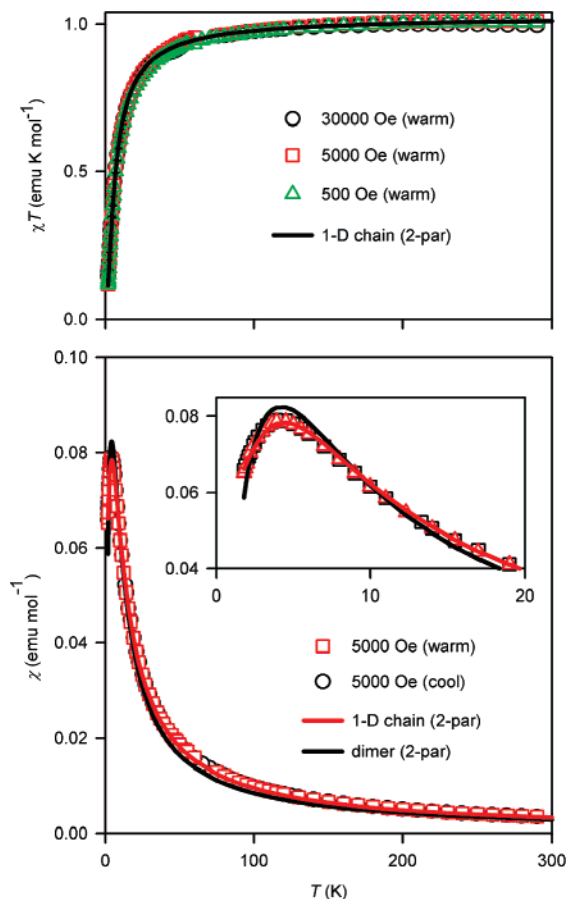
**Figure 9.** SQUID magnetometry for polycrystalline diradical **1**: $\chi T$ vs $T$ plot (top) and $\chi$ vs $T$ plot (bottom) are shown with two variable parameter ($J/k$ and $w$) numerical fits. The values of the optimized parameters (parameter dependence and $R^2$) for the 1-D chain model (eq 3) are as follows: for $\chi T$ vs $T$ fit, $J/k = -3.5$ K, $w = 1.03$ (0.32 and 0.9994), and for $\chi$ vs $T$ fit, $J/k = -3.3$ K, $w = 1.00$ (0.82 and 0.9997). Analogous values for the dimer model (eq S2a, Supporting Information) for the $\chi$ vs $T$ fit are as follows: $J/k = -2.1$ K, $w = 0.87$ (0.74 and 0.9932).

smaller than that for **1**, magnetization may be analyzed in terms of paramagnetic Brillouin $M/M_{sat}$ vs $H/(T - \theta)$ plots with a mean-field parameter $\theta = -1.5$ K, $S \approx 0.9$, and $M_{sat} \approx 0.9 \, \mu_B$.

These data unequivocally indicate that **1** possesses a triplet ground state ($S = 1$) that is exclusively populated at room temperature, that is, the $2J/k$ far exceeds the thermal energy at room temperature ($2J/k \gg 300$ K). Also, this result confirms the high purity of diradical **1**, as already indicated by the $^1$H NMR and EPR spectra (Figures 5 and 6). Because EPR spectra of **2** in solution indicate a negligible amount of $S = \frac{1}{2}$ monoradical (Figure S6, Supporting Information), the low values of $\chi T < 1.0$ emu K mol$^{-1}$ at room temperature and of $M_{sat} < 1.0 \, \mu_B$ are most likely associated with the presence of diamagnetic ($S = 0$) impurities. The diamagnetic impurities (primarily residual solvents) were detected in the $^1$H NMR spectra of **2** (Figure S38, Supporting Information). We conclude that diradical **2** possesses strong paramagnetic properties at room temperature, similar to those of **1**.

For polycrystalline **3**, the $\chi T$ vs $T$ plots are qualitatively different from those for **1** and **2**. A broad maximum with $\chi T \approx 1.0$ emu K mol$^{-1}$ at a temperature of approximately 150–200 K is observed; at $T < 150$ K, the $\chi T$ vs $T$ plot shows a downward turn qualitatively similar to that in **1** and **2** (Figures 10 and S16, Supporting Information). Most importantly, the drop-off in
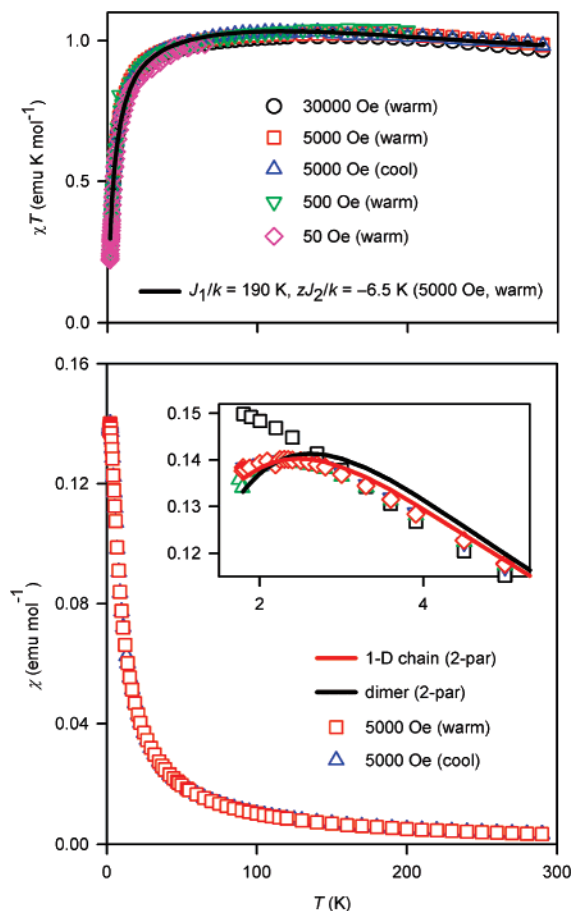


**Figure 10.** SQUID magnetometry for polycrystalline diradical **3**: $\chi T$ vs $T$ (top), $\chi$ vs $T$ (bottom) plots are shown with numerical fits. In the top plot, a three-parameter numerical fit to $\chi T$ vs $T$ (1.8–290 K) at 5000 Oe in warming mode gave the following values of optimized parameters (parameter dependence and $R^2$) for the diradical model (eq 2): $J_1/k = 190$ K, $zJ_2/k = -6.5$ K, and $w = 1.09$ (0.37–0.68 and 0.9933). In the bottom inset plot, two-parameter numerical fits to $\chi$ vs $T$ (1.8–100 K) at 5000 Oe in warming mode are shown. The values of the optimized parameters (parameter dependence and $R^2$) for the 1-D chain model (eq 3) are $J/k = -1.9$ K, $w = 0.86$ (0.86 and 0.9997), and for the dimer model (eq S2a, Supporting Information), $J/k = -1.3$ K, $w = 0.93$ (0.84 and 0.9982).

values of $\chi T$ at $T > 150$ K indicates an increasing thermal population of the singlet excited state at higher temperatures; thus, the ferromagnetic exchange coupling in **3** is weaker than that in **1** and **2**.

The singlet triplet gap for **3** is estimated by numerical fitting of the $\chi T$ vs $T$ data at 5000 Oe to the diradical model (eq 2). The optimized values of the variable parameters are as follows: the singlet triplet energy gap, $2J_1/k \approx 400$–$800$ K; the mean-field correction for an intermolecular antiferromagnetic coupling, $zJ_2/k = -6.5$ to $-6.9$ K;[61] and the weight factor, $w = 1.05$–$1.09$ (Figures 10 and S16, Supporting Information).[1f] The relatively wide range for $2J_1/k$ reflects the difficulty of measuring energy gaps that are comparable to or greater than the thermal energy at room temperature, which is the highest temperature of the measurement of $\chi T$; in such a case, even minor inaccuracies in the correction for diamagnetism would significantly affect the optimized value of $2J_1/k$. Furthermore, the quality of the fits ($R^2 = 0.991$–$0.996$) at lower fields (e.g., 5000 Oe) is rather modest, as the intermolecular antiferromag-

(61) Mean-field correction: Hatfield, W. E.; Weller, R. R.; Hall, J. W. *Inorg. Chem.* **1980**, *19*, 3825–3828.

netic coupling at low temperatures is substantial, making it difficult to account for accurately by an approximate mean-field correction.[62]

$$\chi T = 0.5 w \chi_{\text{dirad}} T / [1 - ((2zJ_2/3k)\chi_{\text{dirad}})]$$

$$\chi_{\text{dirad}} = (1.118wF)/H$$

$$F = [2 \sinh(a)]/\{1 + 2 \cosh(a) + \exp[(-2J_1/k)/T]\}$$

$$a = 1.345(H/T) \qquad (2)$$

These results indicate that the paramagnetic properties of **3** at room temperature are somewhat weakened, compared to those of **1** and **2**. This behavior may be associated with the out-of-plane distortion of the nitroxide moieties in **3** (Figure 3).

**(ii) Chains of $S = 1$ Diradicals.** Because **1**–**3** were determined to possess triplet ground states with strong ferromagnetic coupling, the downward turns at low temperatures in the $\chi T$ vs $T$ plots must be due to intermolecular antiferromagnetic coupling between $S = 1$ diradical molecules. In the $\chi$ vs $T$ plots for **1** and **3**, broad maxima are observed at 4.5 and 2.3 K, respectively;[63] however, the maximum for **3** is only found at low magnetic fields (Figures 9 and 10, inset plots).[64] Two limiting models for such intermolecular antiferromagnetic coupling are considered: (1) 1-D Heisenberg chains of $S = 1$ diradicals (spin-1 chain) and (2) pairs of $S = 1$ diradicals (dimer).

For **1**, the $\chi$ vs $T$ data provide an excellent fit (coefficient of determination, $R^2 = 0.9997$) to a model for a 1-D antiferromagnetic spin-1 chain with two variable parameters: intrachain antiferromagnetic coupling, $J/k = -3.3$ K and a weight factor, $w = 1.00$ (eq 3, Figure 9).[65] The three-parameter fit with an approximate mean-field correction for an interchain coupling ($\theta$) has nearly identical values of $R^2 = 0.9998$, $J/k = -3.3$ K, and $w = 0.99$; because the value of $\theta = -0.03$ K is rather small, compared to our lowest temperature of measurement (1.8 K), it can be estimated as $\theta \approx 0.0 \pm 0.1$ K (eq 3). A recent double-exponential model for 1-D antiferromagnetic spin-1 chains gives a nearly perfect fit ($R^2 = 1.0000$) with a similar value of $J/k \approx -3.5$ K; however, because four variable parameters are used in such model, the fits are overparametrized.[66]

$$\chi_{1D} = \{3/[2k(T - \theta)]\}[(2 + a_1 \times K + a_2 \times K^2)/(3 + b_1 \times K + b_2 \times K^2 + b_3 \times K^3)]$$

$$a_1 = 0.0194, \quad a_2 = 0.777, \quad b_1 = 4.346, \quad b_2 = 3.232,$$
$$b_3 = 5.634, \quad K = -J/kT \quad (3)$$

Analogous two-parameter fits to alternative models, such as pairs of $S = 1$ diradicals (equations S2a and S2b, Supporting Information), are not satisfactory ($R^2 = 0.993$ or $R^2 = 0.994$). The addition of the third parameter for interpair coupling ($\theta$)
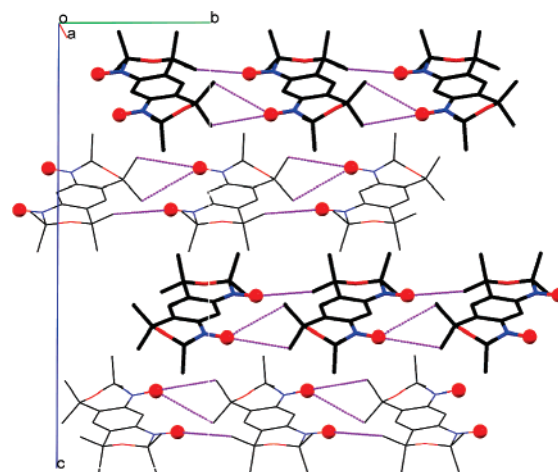


**Figure 11.** Crystal packing of nitroxide diradical **1** showing 1-D chains along the crystallographic *b*-axis. Oxygen atoms (O1 and O2) of nitroxides are shown as red balls. Purple lines correspond the methyl nitroxide contacts, including nonclassical hydrogen bonds, C–H···O–N (C16H···O2 = 2.531 Å). Hydrogen atoms are omitted for clarity.

improves the fit ($R^2 = 0.9995$); however, a relatively large ferromagnetic $\theta \approx 1$ K is obtained. This suggests that the dimer model is not suitable for diradical **1**.

Similar analyses based upon the spin-1 chain and the dimer models are carried out for **3**. Because both models assume $S = 1$ diradicals with an exclusively populated triplet ground state, the numerical fits to the $\chi$ vs $T$ data at 5000 Oe in the warming mode are obtained in the limited temperature range (1.8–100 K), that is, to ensure that the highest temperature (100 K) is considerably lower than $2J_1/k \approx 400$–800 K. Similarly to diradical **1**, the fits to the 1-D spin-1 chain model are superior ($R^2 = 0.9997$) to the fits for the dimer model ($R^2 = 0.9982$) (Figure 10, inset plot). The value of the intrachain antiferromagnetic coupling $J/k = -1.9$ K is about half of that for **1**.

All three diradicals show intermolecular antiferromagnetic coupling, and the magnetic behavior for **1** and **3** is best modeled by 1-D Heisenberg antiferromagnetic spin-1 chains. Further support for the 1-D spin-1 chains is provided by the crystal packing of **1** and **3**, as discussed in the following section.

**Crystal Packing of Diradicals 1 and 3.** Molecules of diradical **1** pack into sheets consisting of 1-D chains of coplanar molecules extending along the crystallographic *b*-axis (Figure 11). Similarly, molecules of **3** pack into sheets consisting of 1-D chains but extending along the crystallographic *a*-axis (Figure 12).

For **1**, short intrachain contacts between the methyl groups and the nitroxide groups are found, for example, the methyl nitroxide C16···2 contacts of 3.502 Å correspond to nonclassical hydrogen bonds, C–H···O–N (C16H···O2 = 2.531 Å). Analogous methyl nitroxide C–H···O–N contacts, such as C14··· O1 of 3.592 Å and C13···O1 of 3.645 Å, somewhat exceed the sum of van der Waals radii.[67]

The hydrogen atoms in C–H···O–N contacts were reported to provide effective exchange coupling pathways in crystalline

(62) For polycrystalline **3** at higher fields such as 30 000 Oe in the warming mode, the fits ($J_1/k = 240$ K, $zJ_2/k = -5.2$ K, $w = 1.05$) are greatly improved, $R^2 = 0.9994$, probably due to the onset of the spin crossover and paramagnetic saturation effects.

(63) Diamagnetic impurities might contribute to the relative weakness of antiferromagnetic interactions in polycrystalline **2**, compared to **1** and **3**.

(64) This field dependence for **3** may indicate the near crossover between the spin states at the higher fields; this phenomenon will require more detailed magnetic studies.

(65) Derivation of equation 2: Meyer, A.; Gleizes, A.; Girerd, J. J.; Verdaguer, M.; Kahn, O. *Inorg. Chem.* **1982**, *21*, 1729–1739.

(66) (a) Souletie, J.; Drillon, M.; Rabu, P.; Pati, S. K. *Phys. Rev. B* **2004**, *70*, 054410-1–6. (b) Numerical fits to the phenomenological expression, developed for *n*-membered rings of spin-1, $\chi T/(Ng^2\mu_B^2/k) = C_{1n} \exp(-W_{1n}/T) + C_{2n} \exp(-W_{2n}/T)$, where $W_2 = 1.793(J/k)$ for infinite *n*, were implemented. For numerical fits to the $\chi$ vs $T$ data of **1**, values for parameter dependencies (0.9968–0.9997) were very close to 1.0, indicating that the fits were overparametrized (i.e., too many variable parameters were used).
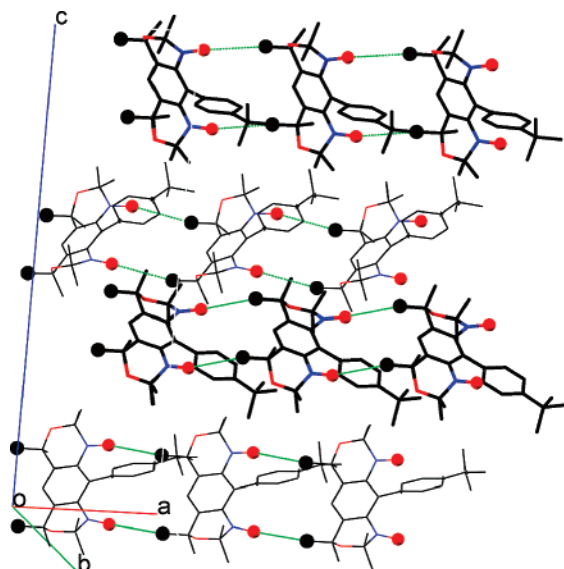
**Figure 12.** Crystal packing of nitroxide diradical **3** showing 1-D chains along the crystallographic *a*-axis. Oxygen atoms (O1 and O2) of nitroxides and carbon atoms (C14 and C16) of the methyl groups are shown as red and black balls, respectively. Green lines indicate the C16H···O2 and C14H···O1 contacts of 3.685 and 3.579 Å, respectively. Hydrogen atoms and disorder are omitted for clarity.

$S = \frac{1}{2}$ nitroxide radicals. For example, the methyl nitroxide C–H···O–N contacts (C···O = 3.35–3.50 Å) in nitronyl nitroxide radicals were found to mediate exchange coupling with $|J/k| \approx 0.5$ K.[68] The magnitude of $|J/k|$ will depend on two factors: (1) the distance (and orientation) between the interacting atoms with spin density, with exponential dependence and (2) the product of the spin densities at the interacting atoms. The three intrachain methyl nitroxide C–H···O–N contacts in diradical **1** are relatively longer than those reported for the nitronyl nitroxides.[68] For all three intrachain methyl nitroxide contacts in **1**, the hydrogen atoms of the methyl groups (C13, C14, C15, and C16) possess substantial positive spin density ($a_H = +0.023$ mT), as indicated by the presence of broadened 12-proton singlet at +24.8 ppm in the ^{1}H NMR spectra of **1** in solution. This spin density is similar in magnitude to that for the methyl groups in nitronyl nitroxides with $a_H = -0.02$ mT.[69] Furthermore, the spin density at the oxygen atom of nitroxide is expected to be 100% greater than that of nitronyl nitroxide. Therefore, the product of spin densities at the interacting hydrogens and oxygens in **1** will be greater by a factor of 2 than that in the nitronyl nitroxide. Three such C–H···O–N contacts provide multiple coupling pathways,[70] thus further amplifying the strength of intrachain exchange coupling in **1**. Because the interacting atoms in **1** have positive spin densities in overlapping (nonorthogonal) orbitals, the intrachain exchange coupling between $S = 1$ diradical molecules should be antiferromagnetic. Thus, the measured value of intrachain $J/k \approx -3$ K is in reasonable agreement with these estimates.

(67) Also, a longer C–H···O–N intrachain contact, with a C5···O2 distance of 3.702 Å between the benzene ring and nitroxide, may be identified in **1**. The hydrogen at C5 of the benzene ring, which could not be observed in ^{1}H NMR spectra of **1** in solution, is expected to possess positive and relatively large spin density.

(68) Cirujeda, J.; Hernàndez-Gasió, E.; Rovira, C.; Stanger, J.-L.; Turek, P.; Veciana, J. *J. Mater. Chem.* **1995**, *5*, 243–252.

(69) ^{1}H NMR spectra of nitronyl nitroxides: Davis, M. S.; Morokuma, K.; Kreilick, R. W. *J. Am. Chem. Soc.* **1972**, *94*, 5588–5592.

(70) Rajca, A.; Rajca, S.; Wongsriratanakul, J. *Chem. Commun.* **2000**, 1021–1022.

To determine dimensionality of the exchange coupling pathways, interchain contacts in **1** are examined. Nonclassical hydrogen bonds are found between alternate chains within each sheet, such as the methyl nitroxide C12···O1 contacts of 3.484 Å (C12H···O1 = 2.536 Å) and the methyl oxazine C12···O3 contacts of 3.612 Å (C12H···O3 = 2.695 Å). However, the hydrogen atoms of the methyl groups adjacent to nitroxides (C11, C12, C17, C18) possess very small negative spin density ($a_H = -0.002$ mT), as indicated by the 12-proton singlet at −0.33 ppm ^{1}H NMR spectra of **1** in solution. This small spin density is more than 1 order of magnitude lower than the spin densities of the hydrogen atoms in the intrachain methyl nitroxide contacts. Also, spin densities at the oxygen atoms of the oxazine rings are expected to be at least an order of magnitude lower than those of the nitroxides. This indicates that such interchain contacts are expected to lead to negligible exchange coupling.

Several interchain contacts between atoms with significant spin densities may be identified, especially the nitroxide–nitroxide contacts in **1**. Such contacts involve relatively large spin densities at interatomic distances of 5.4–6.0 Å. This distance range is similar to the N···N distance of 5–6 Å between two face-to-face oriented nitroxide radicals in the 1,3-alternate calix[4]arene scaffold, for which through-space exchange coupling with $J/k \approx -1$ K was determined.[57] In **1**, however, the relative orientations of the nitroxide moieties do not allow for an effective orbital overlap. Thus, interchain exchange couplings are expected to be significantly less than 1 K, that is, relatively weak, compared to the intrachain antiferromagnetic exchange coupling. Thus, crystalline diradical **1** may be viewed as a 1-D antiferromagnetic spin-1 chain.

For **3**, there are two short intrachain contacts between the methyl groups and the nitroxide groups: the methyl nitroxide C14···O1 and C16···O2 contacts of 3.579 and 3.685 Å, respectively. These two intrachain contacts are analogous to those found in **1**; however, the C–H···O–N distances in **3** are relatively longer than those in **1**. This suggests that the intrachain antiferromagnetic coupling between the $S = 1$ diradicals in **3** is weaker than that in **1**. Similarly to **1**, short interchain methyl nitroxide contacts are found, such as C11···O1 with a distance of 3.675 Å; however, such methyl groups, adjacent to the nitroxides, have relatively small spin densities, and the corresponding interchain exchange coupling should be relatively weak compared to the intrachain exchange coupling. Therefore, the crystal packing of **3** is consistent with the 1-D antiferromagnetic chains of diradicals.

**Antiferromagnetic Spin-1 Chains.** Crystalline diradicals **1** and **3** form highly isotropic chains with relatively weak local anisotropy, $|D/2J| \approx 3 \times 10^{-3}$ and $|D/2J| \approx 5 \times 10^{-3}$, respectively.[71] The local anisotropy for **1** is nearly 2 orders of magnitude less than the local anisotropy ($|D/2J| = 0.2$–0.3) found in the most studied Ni(II)-based spin-1 chains such as NENP and [Ni(1,3-diamino-2,2-dimethylpropane)$_2$($\mu$-N$_3$)](PF$_6$), abbreviated as NDMAP.[31] Therefore, **1** is a promising candidate for the study of the Haldane gap in $S = 1$ 1-D antiferromagnetic Heisenberg chains, with minimum interference from magnetic anisotropy effects. The relatively weak antiferromagnetic coupling, $J/k = -3.3$ K, is associated with a rather small Haldane

(71) For **1** and **3**, $J/k = -3.3$ K and $J/k = -1.9$ K, respectively; $|D/hc| = (1.31$–$1.34) \times 10^{-2}$ cm$^{-1}$ corresponds to approximately 0.019 K.

gap of $0.41 \times (2J/k) \approx 2.7$ K. The interchain coupling ($J'$) can be conservatively estimated at this time as $|J'/J| < 0.1$. Further studies of **1** and **3** at $T < 1.8$ K are required to determine $|J'/J|$ and thus the degree of one-dimensionality.

## Conclusion

We have developed an efficient synthetic methodology for benzobisoxazine-based annelated nitroxide diradicals **1**–**3**. In particular, both **1** and **3** are obtained in good yields as pure crystalline solids. High purity of these diradicals is important for their stability, especially in solution.

Diradicals **1**–**3** possess robust triplet ground states with strong ferromagnetic coupling and good stability at ambient conditions. For **1**, both in solution and in the solid state, the nitroxides are coplanar with *m*-phenylene, and consequently the singlet–triplet energy gaps ($2J$) are exceeding thermal energies of the highest temperatures of magnetic measurements, that is, $2J/k > 200$ K and $2J/k \gg 300$ K, respectively. For **3**, in solution and in the solid state, the nitroxides are not exactly coplanar with *m*-phenylene, because of the steric congestion between the 4-*tert*-butylphenyl group and the oxygens of the nitroxides. Because the distortion from coplanarity is moderate, the singlet–triplet gap remains large both in solution ($2J/k > 200$ K) and in the solid state ($2J/k \approx 400$–$800$ K), though an onset of thermal depopulation of the triplet ground state is detectable near room temperature. Therefore, nitroxide diradicals **1** and **3** possess both strong ferromagnetic coupling and adequate stability, which are important properties required for suitable building blocks for organic magnetic materials as well as for exploration of biomedical applications for $S = 1$ diradicals.

The magnetic behavior for **1** and **3** at low temperature is best modeled by 1-D spin-1 Heisenberg chains with intrachain antiferromagnetic coupling of $J/k = -3.3$ K and $J/k = -1.9$ K, respectively. The antiferromagnetic coupling between the $S = 1$ diradicals may be associated with the methyl nitroxide C−H- - -O contacts, including nonclassical hydrogen bonds. These unprecedented organic antiferromagnetic spin-1 chains are highly isotropic (e.g., $|D/2J| \approx 3 \times 10^{-3}$ for **1**), compared to the most studied Ni(II)-based chains, thus providing novel systems for studies exploring low dimensional magnetism and related areas of fundamental research.

**Supporting Information Available:** General procedures and materials, additional experimental details, discussion of structures of **12** and **13**, X-ray crystallographic files (compounds **1**, **3**, **12**, and **13**) (CIF), and complete ref 42. This material is available free of charge via the Internet at http://pubs.acs.org.

JA0712017